



HAL
open science

Localization with data association

Benoît Desrochers, Luc Jaulin, Sergey Kumkov

► **To cite this version:**

Benoît Desrochers, Luc Jaulin, Sergey Kumkov. Localization with data association. MSCMQ'2018 (Mathematics, Statistics and Computation to Support Measurement Quality 2018), D.I.Mendeleyev Institute for Metrology (Russia); COOMET May 2018, Saint Petersburg, Russia. hal-01832904

HAL Id: hal-01832904

<https://ensta-bretagne.hal.science/hal-01832904>

Submitted on 9 Jul 2018

HAL is a multi-disciplinary open access archive for the deposit and dissemination of scientific research documents, whether they are published or not. The documents may come from teaching and research institutions in France or abroad, or from public or private research centers.

L'archive ouverte pluridisciplinaire **HAL**, est destinée au dépôt et à la diffusion de documents scientifiques de niveau recherche, publiés ou non, émanant des établissements d'enseignement et de recherche français ou étrangers, des laboratoires publics ou privés.

Localization with data association

Benoit Desrochers¹, Luc Jaulin², Sergey Kumkov³

¹DGA Tn, Brest, France

²Lab-STICC, ENSTA Bretagne, Brest, France

³Institute of Mathematics and Mechanics, Russian Academy of Sciences

March 1, 2018

1 Introduction

A feature-based localization problem can be formalized as follows [11]

$$\begin{cases} \dot{\mathbf{x}}(t) = \mathbf{f}(\mathbf{x}(t), \mathbf{u}(t)) & \text{(evolution equation)} \\ \mathbf{g}(\mathbf{x}(t), \mathbf{y}(t)) \in \mathbb{M} & \text{(observation constraint)} \\ \mathbf{x}(0) \in \mathbb{X}_0 & \text{(initial state)} \end{cases} \quad (1)$$

where \mathbf{x} is the unknown state vector, \mathbf{y} an exteroceptive measurement vector, \mathbf{u} a proprioceptive measurement vector. It is known that for all t , $\mathbf{u}(t) \in [\mathbf{u}]$ and $\mathbf{y}(t) \in [\mathbf{y}]$. The set \mathbb{M} is a map which is assumed to be known. Equivalently, the observation constraint can then be written as

$$\exists \mathbf{m}(t) \in \mathbb{M}, \mathbf{m}(t) = \mathbf{g}(\mathbf{x}(t), \mathbf{y}(t)).$$

If we take into account the uncertainty on \mathbf{y} , we can say that the state vector $\mathbf{x}(t)$ is consistent with the interval measurement $[\mathbf{y}](t)$ if

$$\exists \mathbf{m}(t) \in \mathbb{M}, \exists \mathbf{y}(t) \in [\mathbf{y}](t), \mathbf{m}(t) = \mathbf{g}(\mathbf{x}(t), \mathbf{y}(t)).$$

The existential quantification $\exists \mathbf{m}(t) \in \mathbb{M}$ highlights the requirement of solving the so-called *data association problem* which aims at finding which point of the map is associated with the measurement vector \mathbf{y} . If \mathbb{M} is composed with finite number of isolated points., our problem copes with the initial localization problem on a field of point landmarks that are indistinguishable. All measurements have the same aspect and cannot be associated directly with a particular point of the map. This problem frequently arises when acoustic sensors are used to detect underwater environmental features [3].

In this paper, we propose an interval-based method [6] to solve the localization problem efficiently [2] [5].

2 Problem

We consider a robot moving on a plane, the motion of which is described by the state equation

$$\dot{\mathbf{x}}(t) = \mathbf{f}(\mathbf{x}(t), \mathbf{u}(t)) = \begin{pmatrix} \left(\begin{array}{cc} \cos(\psi(\cdot)) & -\sin(\psi(\cdot)) \\ \sin(\psi(\cdot)) & \cos(\psi(\cdot)) \end{array} \right) \cdot \mathbf{v}(\cdot) \\ \omega(\cdot) \end{pmatrix}.$$

The state vector is $\mathbf{x} = (p_x, p_y, \psi)$, where $\mathbf{p} = (p_x, p_y)$ is its position and ψ is its heading. The input vector is $\mathbf{u} = (v_x, v_y, \omega)$, where $\mathbf{v} = (v_x, v_y)$ is the horizontal speed of the vehicle in its own frame, measured for instance with a *Doppler Velocity Log* (DVL) (in case of an underwater robot), and $\omega(\cdot)$ is angular velocity measured by gyroscopes.

For some times $t_i \in \mathbb{T}$, the robot collects the range-bearing vector $\mathbf{y}(t_i) = (\rho(t_i), \varphi(t_i))^T$ to a landmark $\mathbf{m}(t_i) = (m_x(t_i), m_y(t_i))^T$ which belongs to the map \mathbb{M} , composed of a collection of georeferenced points. This leads to the following constraint

$$\exists \mathbf{m} \in \mathbb{M}, \mathbf{m} = \mathbf{g}(\mathbf{x}(t_i), \mathbf{y}(t_i)) \quad (2)$$

with

$$\mathbf{g}(\mathbf{x}(t_i), \mathbf{y}(t_i)) = \begin{pmatrix} p_x(t_i) \\ p_y(t_i) \end{pmatrix} + \rho(t_i) \cdot \begin{pmatrix} \cos(\psi(t_i) + \varphi(t_i)) \\ \sin(\psi(t_i) + \varphi(t_i)) \end{pmatrix}. \quad (3)$$

The localization problem is thus described by the following set of equations:

$$\begin{cases} \dot{\mathbf{x}}(t) = \mathbf{f}(\mathbf{x}(t), \mathbf{u}(t)) \\ \mathbf{m}(t_i) = \mathbf{g}(\mathbf{x}(t_i), \mathbf{y}(t_i)) \\ \mathbf{m}(t_i) \in \mathbb{M} \\ \mathbf{x}(0) \in \mathbb{X}_0 \end{cases} \quad (4)$$

where the trajectory $\mathbf{x}(\cdot)$, and the landmark associated to the measurements taken at time t_i both need to be estimated. This set of equations can be decomposed into:

$$\begin{cases} (i) & \dot{\mathbf{x}}(\cdot) = \mathbf{f}(\mathbf{x}(\cdot), \mathbf{u}(\cdot)) \\ (ii) & \mathbf{m}(t_i) \in \mathbb{M} \\ (iii) & \mathbf{a}_i = \mathbf{m}(t_i) - \mathbf{p}(t_i) \\ (iv) & \alpha_i = \psi(t_i) + \varphi(t_i) \\ (v) & \mathbf{a}_i = \rho \cdot \begin{pmatrix} \cos \alpha(t_i) \\ \sin \alpha(t_i) \end{pmatrix} \end{cases}$$

where a contractor [8] can be defined for each constraint. In particular, the contractor $\mathcal{C}_{\frac{d}{dt}}$ [9] is used to contract the tube $[\mathbf{x}](\cdot)$ with respect to (i). The map \mathbb{M} can be depicted by a subpaving, or by an image, for which a contractor such as the one used in [10] can be used. For any box $[\mathbf{x}] \in \mathbb{IR}^2$, this contractor returns the smallest box which contains all landmarks included in $[\mathbf{x}]$. The constraint (v) corresponds to the polar constraint where the minimal contractor [1] can be used.

3 Test-case

Consider an AUV starting its mission with a huge position uncertainty. This can happen during a dive in deep water [7] or when, for discretion purpose, a long-range transit phase, underwater, is required to reach the working area.

For operational reasons, no external positioning system, such as acoustics beacons or USBL, are deployed. We assume that a part of the mission area has been previously mapped during a previous survey and this area is large enough to be reached by the AUV. The corresponding map \mathbb{M} describing this area is modeled by a set of 280 point landmarks.

Our robot performs a small mission pattern as depicted in Figure 1. It senses its environment using a forward-looking sonar oriented toward the seabed, the scope of which is represented by the blue pie. Every three seconds, it is able to measure the distance and bearing between its pose to some landmarks which range between 10 and 70 meters. The positions of the detected landmarks are depicted by green dots. The 90 red segments represent the measurements. Note that only a small number of mapped landmarks have been detected.

Only the 2D position of the robot and its heading need to be estimated since other state variables (roll, pitch, and altitude, depth) are directly measured.

Assumptions. For simplicity, we consider that fact that only landmarks inside the sonar pie are seen by the AUV is not taken into account by the method. Moreover, in an underwater context, the detected landmarks cannot be distinguished from the others, since for instance, two different rocks can have generally the same aspect and dimension in the sonar image. Moreover, the landmark detection process is sensitive on change in the point of view of the sensor, some landmarks of the map cannot be seen during the survey. Thus, no reliable data associations based on the shape of the landmarks can be assumed. Moreover successive measurements corresponding to the same landmark could be associated by the sonar tracking system. Again, we consider this matching as non reliable and will not be used for the localization.

This example aims at providing a practical illustration of how the constraint propagation methods can be used to:

1. find the trajectory the vehicle
2. solve the data association problem without any combinatorial explosion.

Once these two issues are solved, any classical localization method, such as an EKF [4], can be used to get a more accurate estimate of the trajectory. The filter is initialized with a reliable starting point and only updated with observations which are correctly associated.

4 Results

Given $[\mathbf{x}(0)], \dots, [\mathbf{x}(k_{max})]$ a set of boxes that enclose the state vector of the robot. All are initialized to $\mathbb{R}^2 \times [-\pi, \pi]$. The initial heading is assumed to be

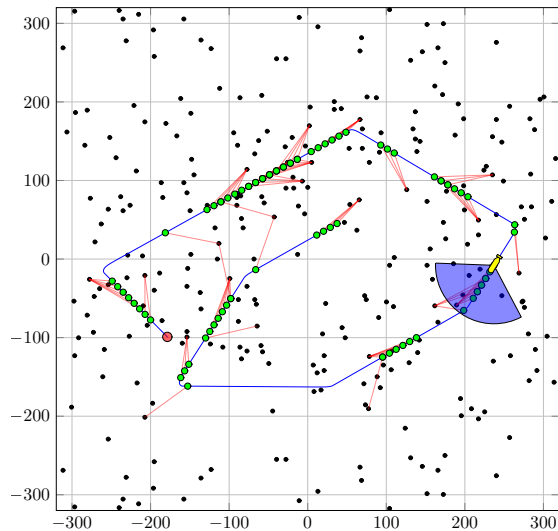


Figure 1: The simulated environment for initial localization. The trajectory of the AUV is depicted by the blue lines. Its starting point is drawn by the red dot. The map is composed of 230 landmarks represented by black dots.

data	description	uncertainty	unit
$\psi(0)$	initial heading	$[-10, 10]$	<i>deg</i>
$\mathbf{v}(t)$	linear speed	$[-0.05, 0.05]^{\times 2}$	<i>m.s</i> ⁻¹
$\omega(t)$	angular velocity	$[-0.001, 0.001]$	<i>deg.s</i> ⁻¹
$\rho(t)$	range	$\rho(t) \cdot [-0.01, 0.01]$	<i>m</i>
$\psi(t)$	azimuth	$[-1, 1]$	<i>deg</i>

Table 1: Uncertainties on data used for the application.

known with an accuracy of ± 10 degrees. Table 1 shows bounds used to quantify error on sensor readings. The map \mathbb{M} is composed of 280 landmarks, and 90 observations have been done during the whole mission.

Figure 4 shows the final trajectory obtained after 12 iterations in less than 1 minute on *i7-5600U CPU@2.60GHz*.

In Table 2, for each iteration, the times needed to contract the whole trajectory are given. This time is constant at each iteration. During the constraint propagation process, the thinner the trajectory is, the smaller the number of landmarks contained in $[\mathbf{m}](t_i)$ is, and vice versa. As an indicator, columns 3 (resp. 4) of Table 2 shows the minimal (resp. maximal) number of landmarks included $[\mathbf{m}](t_i)$ among all measurements. The last column corresponds to the number of correct association, *i.e.*, when $[\mathbf{m}](t_i)$ contains a single landmark. Figure 2 shows diameters of boxes along the trajectory for different iteration which illustrates the constraint propagation process. The constraint propagation methods is shown to be powerful in situations involving a huge number of

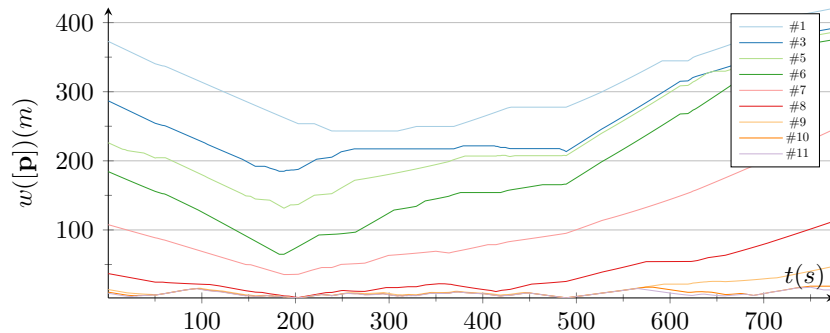


Figure 2: $w([\mathbf{p}])$ with respect to the iteration number.

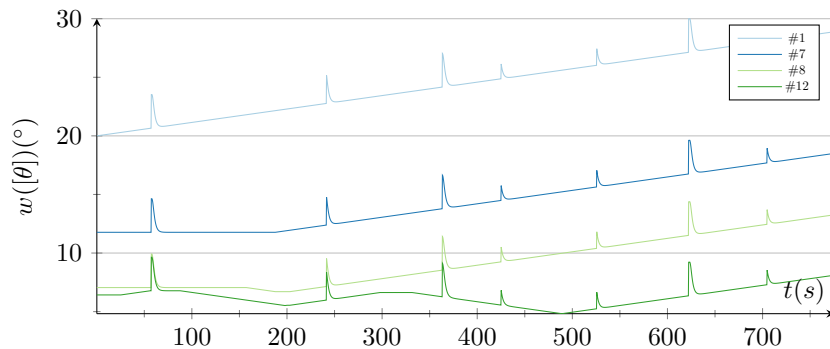


Figure 3: $w([\theta])$ with respect to the iteration number. The peaks in the graph are due to the wrapping effect when the vehicle turns.

possible data association. In comparison, existing method often meet difficulty when both the initial position and the data associations are unknown.

References

- [1] B. Desrochers and L. Jaulin. A minimal contractor for the polar equation; application to robot localization. *Engineering Applications of Artificial Intelligence*, 55:83–92, 2016.
- [2] B. Desrochers, S. Lacroix, and L. Jaulin. Set-membership approach to the kidnapped robot problem. In *IROS 2015*, 2015.
- [3] Maurice F. Fallon, John Folkesson, Hunter McClelland, and John J. Leonard. Relocating underwater features autonomously using sonar-based SLAM. *IEEE Journal of Oceanic Engineering*, 38(3):500–513, 2013.
- [4] L. Jaulin. *Mobile Robotics*. ISTE editions, 2015.

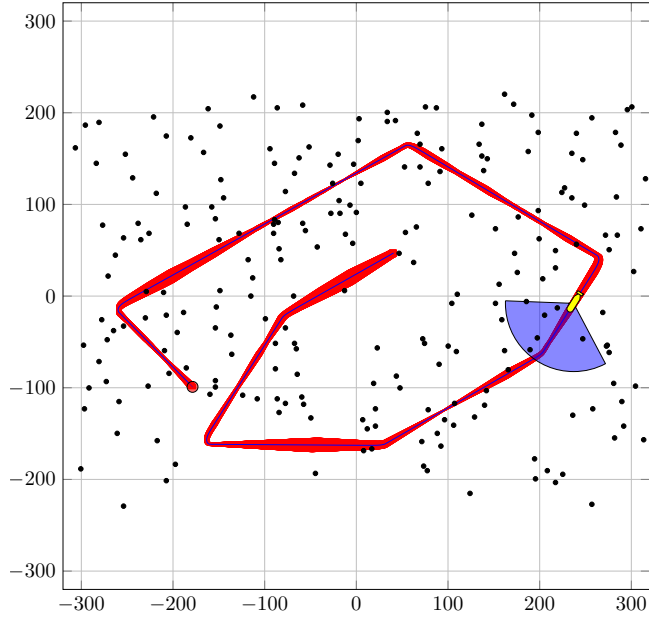


Figure 4: Final trajectory with correct estimation of the initial position and landmarks association. The true trajectory, in blue, belongs the tube in red.

#	time(s)	#min	#max	#ok
1	2.61	202	230	0
2	2.65	27	81	0
3	2.99	22	75	0
4	2.77	15	73	0
5	2.62	11	71	0
6	2.48	4	71	0
7	2.33	2	68	0
8	2.02	1	29	10
9	2.61	1	6	64
10	2.44	1	3	82
11	2.41	1	2	88
12	2.40	1	1	90

Table 2: Time needed to contract the whole trajectory for each iteration. #min (resp. #max) is the smallest (resp. greatest) number of elements of $[\mathbf{m}](t_i)$ among all measurements. #ok denotes the number of good associations. The computing time is nearly constant.

- [5] L. Jaulin and B. Desrochers. Robust localisation using separators. In *COPROD 2014*, 2014.
- [6] Sergey I. Kumkov and Yuliya V. Mikushina. Interval approach to identification of catalytic process parameters. *Reliable Computing*, 19(2):197–214, 2013.
- [7] Stephen McPhail. Autosub6000: A Deep Diving Long Range AUV. *Journal of Bionic Engineering*, 6(1):55–62, mar 2009.
- [8] O. Reynet, L. Jaulin, and G. Chabert. Robust tdoa passive location using interval analysis and contractor programming. In *Radar*, Bordeaux, France, 2009.
- [9] S. Rohou, L. Jaulin, M. Mihaylova, F. Le Bars, and S. Veres. Guaranteed Computation of Robots Trajectories. *Robotics and Autonomous Systems*, 93:76–84, 2017.
- [10] J. Sliwka, F. Le Bars, O. Reynet, and L. Jaulin. Using interval methods in the context of robust localization of underwater robots. In *NAFIPS 2011*, El Paso, USA, 2011.
- [11] S. Thrun, W. Burgard, and D. Fox. *Probabilistic Robotics*. MIT Press, Cambridge, M.A., 2005.